

LOCAL OSCILLATOR CONTRIBUTION TO CARRIER-PHASE MEASUREMENTS IN A GNSS RECEIVER

E. Detoma, L. Bonafede, and P. Capetti

SEPA S.p.A.

Via Andrea Pozzo, 8, 10141 Torino, Italy

Abstract

When performing carrier-phase measurements, the measurement noise affecting the observations reflects two contributions, originating from the thermal noise of the RF signal received at the antenna and from the stability of the local oscillator over the integration time, since normally some form of phase-locked loop (PLL) is used for carrier recovery. The order of the PLL (and the bandwidth) determines the amount of the oscillator contribution to the measurement noise for a given oscillator frequency stability (or, since the integration time is generally less or equal to 1 s, to its phase noise). Therefore, it is important to understand the mechanism by which the local oscillator instability is transferred to the carrier-phase measurement noise and select a proper oscillator to minimize such a contribution.

In the paper, we will address these issues, providing examples that guide the selection of the local oscillator. A practical example of implementation will be discussed, where a low-cost, high-stability OCXO has been disciplined to a Rb frequency standard to provide improved stability over the integration times of interest in order to minimize the noise for carrier-phase recovery.

CARRIER-PHASE TRACKING AND LOCAL OSCILLATOR CONTRIBUTION

In the following, our aim is to define a model, and determine the contributions, for the stochastic errors affecting the performance of the typical GPS (GNSS) receiver. We will consider errors on pseudorange and carrier-phase measurements. Under our assumptions, we will consider the receiver as a measurement instrument, with the target of providing the required measurement (carrier phase or pseudorange) with the best precision.

Considering pseudorange and carrier-phase measurements, we realize that both are affected by the received signal-to-noise ratio, by the receiver implementation (and corresponding implementation losses as respect to theoretical), and by the local oscillator. Let's start by looking at the received signal-to-noise ratio.

RECEIVED SIGNAL-TO-NOISE RATIO

The level of the received signal is a function of the transmitted power and the attenuation over the propagation path between the satellite and the receiver. The transmitted power is assumed constant, while the propagation attenuation will be a function of the relative position between the satellite and the receiver. The following parameters apply:

Table I. GPS transmission parameters.

Parameter	Units	L1 C/A	L1P	L2P ¹
GPS satellite transmitted power	dBm	45.2	45.2	35.2
Code sharing loss	dB	-1.8	-4.8	0
GPS satellite antenna gain	dB	12	12	12

The effective radiated power P_{rad} is the algebraic sum of the above parameters:

$$P_{rad} = P_{tx} - L_{sharing} + G_{antenna}$$

If the geometric distance at the time t is $\rho(t)$, the free-space propagation attenuation L_{free} can be computed using different (but equivalent) formulas, widely available in the literature:

$$(1) \quad L_{free} = 20 \cdot \log_{10}(f \cdot \rho) + 92.45$$

where: f is the carrier frequency, in GHz,
 ρ is the slant range in km, and
 L_{free} is the free-space propagation attenuation, in dB.

An equivalent formula is the following (from Ref. [2], p. 45)

$$(2) \quad L_{free} = \left(\frac{\lambda}{4\pi \cdot \rho} \right)^2$$

where: λ is the RF carrier wavelength, in m,
 ρ is the slant range, in km, and
 L_{free} is the free-space propagation attenuation, as a dimensionless ratio.

The latter can be easily converted in dB as follows:

$$L_{free}(dB) = 10 \cdot \log_{10}(L_{free})$$

In addition to the free-space propagation attenuation, we must consider an additional ≈ 2 dB attenuation due to the interaction of the electromagnetic wave with the atmosphere (absorption). Therefore, the effective received signal power will be the effective radiated power P_{rad} minus the free-space attenuation loss L_{free} minus the atmospheric attenuation $L_{atmosph}$:

$$P_{rx} = P_{rad} - L_{free} - L_{atmosph} \quad (\text{in dBm})$$

Example: For a GPS satellite, assume an effective radiated power of 45.2 dBm,

¹ Without L2C

a code sharing loss of -1.8 dB, and an antenna gain of 12 dB: the effective radiated power is 55.4 dBm.

Given a slant range of 25149.567 km, at the L1 frequency (1575 MHz) the free-space propagation attenuation is -184.406 dB, and the received signal power level is -129.006 dBm, to be further reduced by \approx -2 dB because of atmospheric attenuation, so that the effective received signal level at the receiver antenna will be -131.006 dBm.

The receiving antenna detects the signal with a gain that is a function of the polar radiation diagram of the antenna itself. If the elevation angle for the satellite is E, the corresponding antenna gain is $G_{ant}(E)$ (we assume this is a function of E only). Therefore, from geometric considerations based on the relative position of satellite and receiver, E can be computed and $G_{ant}(E)$ determined.

The input signal power to the receiver P_{in} at the antenna output² is again the algebraic sum of the received signal level P_{rx} in dBm and if the antenna gain, in dB:

$$P_{in} = P_{rx} + G_{ant}(E)$$

Example: following the previous example, assuming $P_{rx} = -131.006$ dBm and an antenna gain of -3 dB at 5° elevation, the signal power P_{in} at the output of the receiving antenna will be $P_{in} = -134.006$ dBm.

The noise at the input of the receiver is a complex function of many parameters, including the antenna noise temperature, the attenuation introduced by the cable connecting the antenna to the receiver, the gain and noise figure of the low-noise amplifier (LNA) that follows the antenna, and the noise figure of the receiver itself. To simplify, we can consider a single parameter, generally provided by the manufacturer, that characterizes the noise performance of the receiver with respect to an ideal receiver.

This parameter is the receiver noise equivalent temperature T_{noise} , and we assume³, for instance, that $T_{noise} = 238.941$ °K. This value is everything we need, assuming that the noise temperature of the antenna, the noise figure of the LNA, and the length and characteristics (attenuation) of the antenna cable remain constant.

From the equivalent noise temperature T_{noise} , it is straightforward to compute the equivalent noise power spectral density P_{noise} , that can be regarded as the equivalent noise power in a unit bandwidth (1 Hz):

$$\begin{aligned} P_{noise} &= 10 \cdot \log_{10}(T_{noise} \cdot k) \quad \text{in dBW} \\ P_{noise} &= 10 \cdot \log_{10}(T_{noise} \cdot k) + 30 \quad \text{in dBm} \end{aligned}$$

where $k = 1.3807 \cdot 10^{-23}$ is the Boltzmann constant. For $T_{noise} = 238.941$ °K, the corresponding noise power spectral density is -174.816 dBm/Hz.

Now, the ratio C/N_0 (in dB/Hz) between the signal (carrier) and the noise will be simply the difference between the available signal power $P_{in} = -134.006$ dBm and the noise power $P_{noise} = -174.816$ dBm/Hz:

² For the time being, we consider the antenna output as the input of the receiver, assuming that the cable connecting the antenna to the receiver as an integral part of the receiver itself. The reason will be apparent in the discussion that follows.

³ This is a value measured for a very good geodetic-quality receiver, and applies both to L1 and L2.

$$\begin{aligned} C/N_0 &= P_{in} - P_{noise} \\ &= -134.006 + 174.816 = 40.81 \text{ dB/Hz} \end{aligned}$$

For an ideal receiver, this value is not degraded by the receiver implementation. In practice, a real receiver introduces implementation losses with respect to the mechanization of an ideal receiver, a degradation which is due to losses in the amplification, mixing, and sampling circuits. This additional degradation is known as implementation loss L_{impl} and results in a further degradation in the C/N_0 ratio. Assume that $L_{impl} = -3$ dB. Then the effective C/N_0 ratio will be less than theoretical because of this implementation loss:

$$\begin{aligned} (C/N_0)_{\text{effective}} &= P_{in} - P_{noise} - L_{impl} \\ &= 37.81 \text{ dB/Hz} \end{aligned}$$

This is the value of C/N_0 (in dB/Hz) that we will use in the following. For a given receiver, where the majority of the above-mentioned parameters can be considered as constant, this value will be a function of the slant range and elevation angle (for the antenna gain).

ESTIMATION OF THE NOISE AFFECTING THE CARRIER-PHASE MEASUREMENTS

The noise affecting the carrier-phase measurements can be estimated by generalizing the theory of phase-locked loops (PLLs), since we can consider the receiver as using some form of a Costas loop to reconstruct the suppressed carrier. It can be shown that other methods (based, for instance, on the squaring of the signal to recover the suppressed carrier) produce theoretically equivalent results, and therefore the results that are presented in the following are implementation-independent (except for the implementation losses introduced by the practical implementation, obviously).

The noise affecting the phase measurements on the recovered carrier consists in the sum of two contributions, the thermal noise affecting the RF input signal and the stability of the local oscillator (since any phase measurement is always relative):

$$\sigma_{phase} = \sqrt{\sigma_{thermal}^2 + \sigma_{LO}^2}$$

The two contributions will be separately analyzed.

CONTRIBUTION DUE TO THE STABILITY OF THE LOCAL OSCILLATOR

The time error (jitter) Δt produced over an interval τ because of the instability of the local oscillator is:

$$\Delta t(\tau) = \tau \cdot \sigma_y(\tau) \quad (\text{in seconds})$$

where $\sigma_y(\tau)$ is a measure of the frequency instability of the oscillator expressed as the Allan variance of the fractional frequency fluctuations⁴. For a phase-locked loop, the characteristic time interval τ can be considered as the inverse of the loop bandwidth B_L :

$$\tau = \frac{1}{B_L}$$

where we are, for the time being, neglecting the loop filter actual transfer function and considering an ideal response:

⁴ I.e.: $\Delta f/f$.

$$\Delta t(\tau) = \frac{\sigma_y(\tau)}{B_L}$$

Since Δt is expressed in seconds, we transform to radians, considering that:

$$\frac{\Delta t}{P} = \frac{\Delta\phi}{2\pi}$$

where $\Delta\phi$ is the phase (angle) error corresponding to Δt , P is the period of the signal and $f = \frac{1}{P}$ is the frequency (carrier) of the signal. Since we consider the Allan variance (or its square root, the Allan deviation) as a measure of the fractional frequency $\frac{\Delta f}{f}$ instability of the oscillator, its value is not affected by frequency multiplication or phase-locked circuits that up- or down-convert the frequency of the local oscillator, except for implementation losses that we will consider negligible in this particular case and for the time being. Then:

$$\Delta t = \frac{P \cdot \Delta\phi}{2\pi} = \frac{\Delta\phi}{2\pi \cdot f}$$

and, replacing in the previous equation:

$$\Delta\phi = \frac{2\pi \cdot f \cdot \sigma_y(\tau)}{B_L} \quad (\text{in radians})$$

and finally transforming in degrees, since: $\Delta\phi[\text{deg}] = \frac{360}{2\pi} \cdot \Delta\phi[\text{rad}]$:

$$\begin{aligned} \Delta\phi &= \frac{360}{2\pi} \cdot \frac{2\pi \cdot f \cdot \sigma_y(\tau)}{B_L} = \\ &= 360 \cdot \frac{f \cdot \sigma_y(\tau)}{B_L} \end{aligned} \quad (\text{in degrees})$$

To obtain the equivalent noise in mm, assuming $c \approx 3 \cdot 10^8 \text{ m} \cdot \text{s}^{-1}$, $\frac{\Delta\phi[\text{deg}]}{360^\circ} = \frac{\Delta x}{\lambda}$, where λ is the wavelength, since $\lambda = \frac{c}{f}$, we obtain:

$$\begin{aligned} \Delta x &= \frac{\lambda}{360} \cdot \Delta\phi = \frac{\lambda}{360} \cdot 360 \cdot \frac{f \cdot \sigma_y(\tau)}{B_L} = \\ &= \frac{c}{f} \cdot \frac{f \cdot \sigma_y(\tau)}{B_L} = \frac{c \cdot \sigma_y(\tau)}{B_L} \end{aligned}$$

which is equivalent to:

$$\Delta x = \frac{\lambda}{360} \cdot \Delta\phi = \frac{\lambda}{360} \cdot 360 \cdot \frac{f \cdot \sigma_y(\tau)}{B_L} = \frac{c}{f} \cdot \frac{f \cdot \sigma_y(\tau)}{B_L} = \frac{c \cdot \sigma_y(\tau)}{B_L}$$

We have so far considered the ideal behavior of a stand-alone local oscillator over a suitable time interval τ . In practice, the phase-locked loop performances improve significantly for a second or third order loop, where we have:

Table II. Noise for second- and third-order loops.

Order of the loop	Noise [degrees]	Noise [mm]
Third-order	$\Delta\phi = 160 \cdot \frac{f \cdot \sigma_y(\tau)}{B_L}$	$\Delta x = \frac{\lambda}{360} \cdot 160 \cdot \frac{f \cdot \sigma_y(\tau)}{B_L}$ $= \frac{c}{360 \cdot f} \cdot 160 \cdot \frac{f \cdot \sigma_y(\tau)}{B_L}$ $= \frac{4}{9} \cdot \frac{c \cdot \sigma_y(\tau)}{B_L}$
Second-order	$\Delta\phi = 144 \cdot \frac{f \cdot \sigma_y(\tau)}{B_L}$	$\Delta x = \frac{144}{360} \cdot \frac{c \cdot \sigma_y(\tau)}{B_L} =$ $= 0.4 \cdot \frac{c \cdot \sigma_y(\tau)}{B_L}$

Example: Assume that the phase measurements are obtained with a loop bandwidth $B_L = 1$ Hz. If for $\tau = 1$ s the stability of the local oscillator, as fractional frequency deviation (Allan deviation) is $\sigma_y(\tau) = 5 \cdot 10^{-12}$, then the contribution to the noise of the carrier phase measurement due to the local oscillator is $\Delta x = 0.67$ mm for a third-order loop.

CONTRIBUTION DUE TO THE THERMAL NOISE

For a high-performance, geodetic-quality receiver, the carrier recovery loop and associated phase measurement circuits will produce a measurement time series affected by a jitter that can be estimated as follows:

$$\sigma_{thermal} = \frac{360}{2\pi} \cdot \sqrt{\frac{B_\phi}{C/N_0} \cdot \left(1 + \frac{1}{2 \cdot C/N_0 \cdot T}\right)}$$

in degrees, where:

- B_ϕ is the loop bandwidth (assume for the moment $B_\phi = 1$ Hz)
- C/N_0 is the signal (carrier)-to-noise power ratio, expressed as a ratio. To obtain this value from the value in dB obtained previously, as a function of slant range and elevation, use the relationship

$$C/N_0 = 10^{\frac{C/N_0 [dB/Hz]}{10}}.$$

Therefore, if $C/N_0 = 37.81$ dB, we have as a ratio between the signal and noise power $C/N_0 = 6039.49$ and this is the value that should be used in the above equation.

- T is the predetection integration time [in s]; for the majority of GPS commercial receivers, this can be considered as $T = 20$ ms.

Example: Following the previous example and considering the values

obtained so far, we have: $C/N_0 = 37.81 \text{ dB/Hz}$, $T = 20 \text{ ms}$, and $B_\phi = 1 \text{ Hz}$. Under these assumptions, the thermal noise contribution to the jitter affecting the carrier-phase measurements is $\Delta x = 0.39 \text{ mm}$. Notice how this value is significantly less to the contribution due to the local oscillator with a frequency stability of $\sigma_y(\tau) = 5 \cdot 10^{-12}$ at 1 s, that is already a very good frequency stability. Adding the two contributions, respectively, due to the local oscillator instability and to the thermal noise, the resulting jitter affecting the carrier-phase measurements results in 0.773 mm, where the dominant term is due to the local oscillator.

PSEUDORANGE MEASUREMENTS NOISE (CODE, SS-PRN)

Two models will be considered: the first to estimate the theoretical performance that can be obtained from the GPS code measurements using a Minimum Value Unbiased Estimator (MVUE) and the second to estimate the performance that can be obtained by a digital non-coherent Early-minus-Late phase-locked loop.

MINIMUM VALUE UNBIASED ESTIMATOR [MVUE]

Make use of the following relationship (cf. Ref. [6], Eq. 2-21, p. 137):

$$\sigma_{code,MVUE}[m] = \frac{1}{4} \cdot \sqrt{\frac{2 \cdot T}{k \cdot \frac{C}{N_0} \cdot W_c}} \cdot c$$

where:

W_c is the signal (code) bandwidth ($W_c = 1.024 \text{ MHz}$ for a typical receiver)

C/N_0 is the signal (carrier)-to-noise power ratio, expressed as a ratio. To obtain this value from the value in dB obtained previously, as a function of slant range and elevation, use the relationship

$$C/N_0 = 10^{\frac{C/N_0[\text{dB}/\text{Hz}]}{10}}$$

Therefore, if $C/N_0 = 37.81 \text{ dB}$ we have as a ratio between the signal and noise power $C/N_0 = 6039.49$ and this is the value that should be used in the above equation.

T is the integration (observation) time for the signal [in s]; let $T = 0.02 \text{ s}$

k is a constant:

- $k = 512 \cdot 10^3$ for the GPS C/A code
- $k = 512 \cdot 10^4$ for the GPS P code

c is the speed of propagation of the light “in vacuum.”

W_c , k and T can be considered constant parameters, while C/N_0 should be computed from the slant range and the elevation, the latter to keep into account the antenna gain.

Example: Following the previous example, let $C/N_0 = 37.81 \text{ dB/Hz}$, $W_c = 1.024 \text{ MHz}$, $T = 0.02 \text{ s}$, and $k = 512 \cdot 10^3$ (C/A code); the jitter affecting the pseudorange measurements is 0.27 m.

DIGITAL NON-COHERENT “EARLY-MINUS-LATE” PHASE-LOCKED LOOP

The equation (cf. Ref. [1], p. 14) models the jitter standard deviation for a digital non-coherent “Early-minus-Late” phase-locked loop:

$$\sigma_{DLL} = \sqrt{\frac{B_L \cdot d}{2 \cdot \frac{S}{N_0}} \cdot \left(1 + \frac{2}{(2-d) \cdot \frac{S}{N_0} \cdot T} \right)}$$

where:

B_L is the loop bandwidth (let $B_L = 10$ Hz)

S/N_0 is the signal (carrier)-to-noise power ratio, expressed as a ratio. To obtain this value from the value in dB obtained previously, as a function of slant range and elevation, use the relationship

$$C/N_0 = 10^{\frac{C/N_0 [dB/Hz]}{10}}.$$

Therefore, if $C/N_0 = 37.81$ dB, we have as a ratio between the signal and noise power $C/N_0 = 6039.49$ and this is the value that should be used in the above equation.

T is the predetection filter integration time [in s]; let $T = 20$ ms unless otherwise specified

d is the correlator resolution, expressed in chips of the PRN code.

Multiplying the above result for the chip period and for the value of the speed of light in free-space we obtain the standard deviation on the pseudorange measurement⁵:

$$\sigma_p[m] = \sigma_{DLL} \cdot T_c \cdot c = T_c \cdot c \cdot \sqrt{\frac{B_L \cdot d}{2 \cdot \frac{S}{N_0}} \cdot \left(1 + \frac{2}{(2-d) \cdot \frac{S}{N_0} \cdot T} \right)}$$

where: T_c is the chip period ($T_c = 1/1.024$ MHz for the C/A code)

c is the speed of light in free space.

Example: Following the previous example and using the same parameters, $C/N_0 = 37.81$ dB/Hz, $T_c = 1/1.024$ MHz, let $B_L = 10$ Hz and $d = 0.14$ (C/A code); then the jitter affecting the C/A code pseudorange measurements is 3.18 m.

The above equation should not be used for P-code measurements on commercial geodetic receivers, since it will certainly provide optimistic results. The decrease in the chip period ($T_c = 1/10.24$ MHz for the P code) is only partially compensated by the change in S/N_0 ratio, generally around -3 dB at low elevations, while the equation does not account⁶ for the implementation losses due to "code-less" correlation techniques used for P1. For P2 there is a significative increase in the implementation losses, as will be shown in the next section.

IMPLEMENTATION LOSSES FOR CODELESS P2 TRACKING

A description of the existing techniques is given in the excellent paper by K. T. Woo [5]. The implementation loss for the most commonly used techniques is given in (Figure 1). The "Z-tracking" appears to be the most efficient technique among those considered.

⁵ Cf. also Ref. [0], p. 169.

⁶ Consider that, for P1, the carrier can be recovered from the C/A code recovery loop; this is not possible for P2 on L2 without L2C.

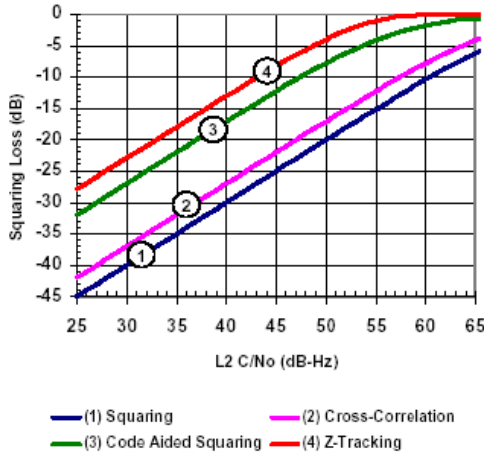


Figure 1. Implementation loss in P2 codeless recovery (from Ref. [5]).

For the “Z-tracking” technique, between 25 and 50 dB-Hz the loss appears sufficiently linear to justify a linear approximation to model it:

$$Loss_{L2} = -53 + C / N_0 \text{ [in dB]}$$

where both $Loss_{L2}$ and C/N_0 are expressed in dB. The jitter affecting the carrier-phase and the code measurements can be estimated using the previous equations by further degrading the implementation loss of the receiver by the contribution due to $Loss_{L2}$.

GALILEO CODE TRACKING

L1 BOC(1,1) CODE ANALYSIS

Galileo performances are expected to be markedly improved at L1 by the use of the BOC (1,1)⁷ versus the BPSK modulation used by the GPS C/A code at L1. The advantage is in that, while the useful bandwidth is the same, the BPSK spectrum is centered around the carrier, while the BOC spectrum is split apart from the suppressed carrier, effectively occupying a bandwidth extending from 1 to 2 MHz from the carrier.

The approximate expression for the expected noise at L1 for Galileo BOC (1,1) signal as given in Refs. [7] and [8] as:

$$(3) \quad \sigma_c = T_c \cdot \frac{1}{\sqrt{3}} \cdot \sqrt{\frac{B_L \cdot d}{2 \cdot \frac{C}{N_0}}} \cdot \sqrt{1 + \frac{2}{(2-d) \cdot \frac{C}{N_0} \cdot T}}$$

A close inspection of Eq. (3) shows that the equation is identical to the GPS BPSK performance (except for the term c , which simply translates the timing uncertainty into ranging uncertainty) and the factor $\frac{1}{\sqrt{3}}$, which represents the

⁷ Now is MBOC.

expected improvement of the BOC Galileo modulation over the BPSK GPS modulation. In practice, we expect an even greater improvement because of the added transmitted RF power from the Galileo satellites, which contributed to an improved C/N₀ ratio. But, as a minimum, we can safely assume just an improvement in performances of a factor $\frac{1}{\sqrt{3}} = 1.7$.

E5A SIGNAL ANALYSIS

The expression for the pseudo-range code noise on E5a is slightly more complex than for the BOC(1,1) at L1. Again, from Refs. [7] and [9], the precision of the measurements is given as:

$$(4) \quad \sigma_c = T_c \cdot \sqrt{\frac{B_L}{2 \cdot \frac{C}{N_0}} \cdot \left[\frac{1}{b} + \frac{b}{\pi-1} \cdot \left(d - \frac{1}{b} \right)^2 \right] \left[1 + \frac{2}{(2-d) \cdot \frac{C}{N_0} \cdot T} \right]}$$

As you can notice from a close inspection of Eqs. (3) and (4), the term d at the numerator of the first term under square root has been replaced by the following term:

$$\left[\frac{1}{b} + \frac{b}{\pi-1} \cdot \left(d - \frac{1}{b} \right)^2 \right]$$

where b is the normalized front-end bandwidth and we assume as usual that $B_L \cdot T \ll 1$.

The conclusions of the previous analysis are summarized in Table III. The values reported are those computed in the numerical example used in the previous sections, corresponding to a worst-case example (low elevation).

It is clear that the selection of the local oscillator is critical to the precision in the carrier-phase measurements; notice that, even with a stability of $5 \cdot 10^{-12}$, the dominant contribution to the carrier-phase measurement noise remains the local oscillator. The contributions (local oscillator and thermal noise) become equivalent only for a stability close to $1 \cdot 10^{-12}$, where both are in the order of 0.4 mm. Therefore, it is very important to ensure the stability of the local oscillator under these circumstances not to degrade, as far as possible, the precision of the measurements.

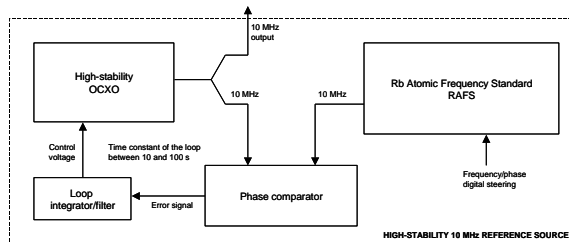


Figure 2. High-stability 10 MHz reference source (with improved short-term stability in the 10^{-12} region ($\tau = 0.1$ to 10 s)).

A HIGH-STABILITY LOCAL OSCILLATOR FOR OPTIMUM SIGNAL TRACKING

From the previous discussion, it is clear that the local oscillator stability affects the performance and the measurement noise of a geodetic-quality GNSS receiver. In particular, SEPA has been tasked, under contract of Thales Alenia Space Italy, in developing high short-term stability and low phase-noise references (Figure 7) based on the steering of a low-noise OCXO to a Rb frequency standard (Figure 2), to provide a high-performance local

oscillator for GNSS receivers applications within the Galileo Test Range (GTR) in Rome.

The phase-locked loop is used to combine the medium-term stability of the Rb oscillator (this is a high-performance SpectraTime LPFRS-01 Rb oscillator; see Figure 3) with the excellent short-term stability of a Morion MV89 double-oven OCXO (Figure 4).

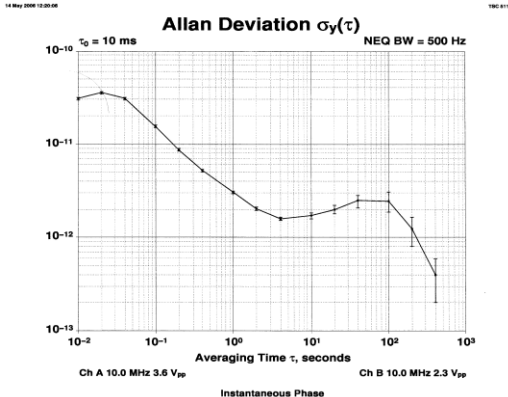


Figure 3. Rb oscillator, 10 MHz output, stand-alone.

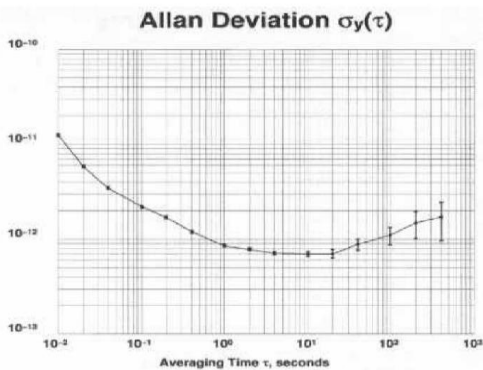


Figure 4. MV89 OCXO, 10 MHz output stability, stand-alone.

The optimum locking point, designed by an appropriate choice of the loop bandwidth, is at the point in which the stability of the RB oscillator alone intersects the stability of the OCXO oscillator alone (Figure 5).

In practice, the point must be selected by assuming also the degradation in stability of the two oscillators due to the environmental conditions, and will be generally for a shorter time constant than the one dictated by stability in optimum conditions alone. This is to account for the inevitable degradation in frequency stability when the oscillators operate in real-world conditions.

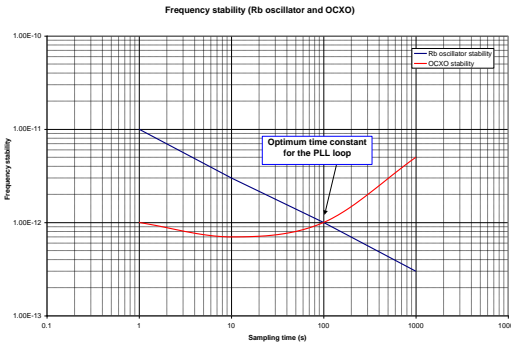


Figure 5. Frequency stability for a Rb oscillator and a high-stability OCXO.

The result is the stability performance for the combined oscillator shown in Figure 6. The frequency stability improvement is dramatic with respect to the Rb alone in the region for $t < 1$ s. From 100 ms to 1 s, the stability of the 10 MHz output of the combined oscillator is below $4 \cdot 10^{-12}$. The data were taken at INRIM in Torino against an H-maser, so the contribution of the local reference is negligible and the plot shows the actual stability of the combined OCXO+Rb oscillator only.

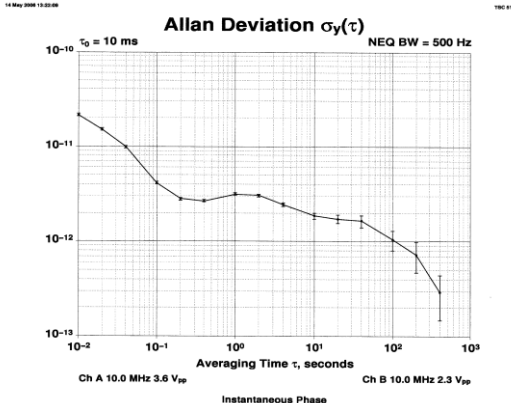


Figure 6. OCXO locked to Rb.

CONCLUSIONS

The optimum selection of the local oscillator for a high-quality GNSS receiver is very important and extremely critical to reduce the noise and improve the precision of carrier-phase measurements. When a single oscillator does not provide all the required characteristics, the solution can still be found by combining more than one oscillator to achieve the desired results.

The original equipment has been developed with analog circuitry because of an extremely stringent deadline in the procurement. Work is continuing to develop an advanced, redundant version with digital control and more features.

ACKNOWLEDGMENTS

The author is grateful to Thales Alenia Space Italy for the initial stimulus to investigate the properties of the local

oscillator for high-quality geodetic receivers (Thales Alenia Space Italy, Milan and Turin plants, in support to the ESA GOCE satellite mission) and for the support provided (Thales Alenia Space, Rome) by funding this development in the framework of the GTR activities, to the colleagues of INRIM for the help in testing the equipment and to the colleagues in SEPA for the help provided in assembling the instruments.

E. Detoma wishes to dedicate this work to the memory of his mother Anna, who passed away while he was writing it.

REFERENCES

- [1] L. Marradi, "LAGRANGE receiver: Raw Measurements and Navigation Data Processing Analysis Summary," LABEN Technical Note TL17856.
- [2] M. S. Grewal, L. R. Weill, and A. P. Andrews, 2001, **Global Positioning Systems, Inertial Navigation and Integration** (Wiley Interscience, New York).
- [3] "Invitation to tender for SSTI for GOCE Satellite: answers to request for clarification (2)," LABEN fax no. LA-OF-MK-TF-0878-01 (5 October 2001).
- [4] E. D. Kaplan, ed., 1996, **Understanding GPS: Principles and Applications** (Artech House Telecommunications Library).
- [5] K. T. Woo, 1999, "Optimum Semi-Codeless Carrier Phase Tracking of L2," in Proceedings of the ION GPS Meeting, 14-17 September 1999, Nashville, Tennessee, USA (Institute of Navigation, Alexandria, Va.), pp. 289-305.
- [6] D. Weill, 1994, "C/A Code Pseudo-ranging Accuracy – How Good Can It Get?" in Proceedings of ION GPS, 20-23 September 1994, Salt Lake City, Utah, USA (Institute of Navigation, Alexandria, Va.), pp. 133-141.
- [7] N. Gerein, M. Olynik, M. Clayton, J. Auld, and T. Murfin, 2005, "A dual frequency L1/E5a Galileo Test receiver," in Proceedings of the European Navigation Conference GNSS 2005, 19-22 July 2005, Munich, Germany.
- [8] N. Gerein, M. Olynik, and M. Clayton, 2004, "Galileo BOC(1,1) prototype receiver development," in Proceedings of ION GNSS Meeting, 21-24 September 2004, Long Beach, California, USA (Institute of Navigation, Alexandria, Virginia), pp. 2604-2610.
- [9] J. W. Betz, 2000, "Design and performance of code tracking for the GPS M-code signal," in Proceedings of ION GPS, 19-22 September 2000, Salt Lake City, Utah, USA (Institute of Navigation, Alexandria, Virginia).

Table III. Summary of contributions to the noise affecting the carrier-phase and code measurements (GPS receiver).

Measurement	Contributions	Measurement precision (jitter)	Dominant contribution
Carrier phase	Local oscillator stability $\sigma_y(\tau) = 5 \cdot 10^{-12}$	0.7 mm	Stability of the local oscillator
	Signal thermal noise - C/N ₀ = 37.810 dBm/Hz	0.39 mm	
Pseudorange (C/A code)	Local oscillator stability $\sigma_y(\tau) = 5 \cdot 10^{-12}$	Negligible	Thermal noise
	Signal thermal noise - C/N ₀ = 37.810 dBm/Hz	3 ÷ 4 m for “Early-minus-Late” correlator	



Figure 7. High-stability frequency reference, inner view showing Rb and OCXO.